A&A 508, 603–614 (2009)
DOI: 10.1051/0004-6361/200913021
© ESO 2009

Astronomy & Astrophysics

Radio and spectroscopic properties of miniature radio galaxies: revealing the bulk of the radio-loud AGN population⋆

R. D. Baldi[1] and A. Capetti[2]

[1] Universitá di Torino, via P. Giuria 1, 10125 Torino, Italy
e-mail: baldi@oato.inaf.it
[2] INAF – Osservatorio Astronomico di Torino, Strada Osservatorio 20, 10025 Pino Torinese, Italy
e-mail: capetti@oato.inaf.it

Received 30 July 2009 / Accepted 22 September 2009

ABSTRACT

We explore radio and spectroscopic properties of a sample of 14 miniature radio galaxies, i.e. early-type core galaxies hosting radio-loud AGN of extremely low radio power, 10^{27-29} erg s^{-1} Hz^{-1} at 1.4 GHz.
Miniature radio galaxies smoothly extend the relationships found for the more powerful FR I radio galaxies between emission line, optical and radio nuclear luminosities to lower levels. However, they have a deficit of a factor of ∼100 in extended radio emission with respect to that of the classical example of 3CR/FR I. This is not due to their low luminosity, since we found radio galaxies of higher radio core power, similar to those of 3CR/FR I, showing the same behavior, i.e. lacking significant extended radio emission. Such sources form the bulk of the population of radio-loud AGN in the Sloan Digital Sky Survey. At a given level of nuclear emission, one can find radio sources with an extremely wide range, a factor of ≳100, of radio power.
We argue that the prevalence of sources with luminous extended radio structures in flux limited samples is due to a selection bias, since the inclusion of such objects is highly favored. The most studied catalogues of radio galaxies are thus composed by the minority of radio-loud AGN that meet the physical conditions required to form extended radio sources, while the bulk of the population is virtually unexplored.

Key words. galaxies: active – galaxies: elliptical and lenticular, cD – galaxies: nuclei – galaxies: jets – galaxies: evolution

1. Introduction

The presence of a radio source represents the most common manifestation of nuclear activity in early type galaxies. These sources are associated with a fraction as high as 40% of all bright elliptical and lenticular galaxies (e.g. Sadler et al. 1989; Auriemma et al. 1977). Due to the steepness of their luminosity function, most radio sources are of low luminosity. The interest in the properties of these objects lies in the fact that they sample an essentially unexplored regime for radio loud AGN (hereafter RLAGN) and they effectively close the gap between active and quiescent galaxies.

Balmaverde & Capetti (2006) considered a sample of low luminosity radio sources (∼10^{26-29} erg s^{-1} Hz^{-1} at 5 GHz) well suited for such a study. They are hosted by early-type galaxies selected on the basis of the presence of a shallow core in their host surface brightness profiles, defined as "core" galaxies (hereafter CoreG). They used HST and Chandra data to isolate their optical and X-ray nuclear emission, showing that CoreG invariably host radio-loud nuclei, with an average radio loudness parameter of $R = L_{5\ \mathrm{GHz}}/L_{\mathrm{B}} \sim 4000$, similar to the value measured for FR I radio galaxies. Their optical and X-ray nuclear luminosities correlate with the radio-core power, smoothly extending the analogous correlations found for FR I low luminosity radio galaxies (Chiaberge et al. 1999; Balmaverde et al. 2006) toward even lower power, by a factor of ∼1000, covering a combined range of 6 orders of magnitude.

The similarities between CoreG and FR I include the distributions of black hole masses, host galaxy luminosities, and also the properties of the surface brightness profiles (de Ruiter et al. 2005). This indicates that they are drawn from the same population of early-type galaxies.

The level of activity in these sources is closely related to the accretion rate of hot gas derived analyzing Chandra images. Balmaverde et al. (2008) considered a sample of 44 galaxies (CoreG and FR I) and found that the accretion power correlates linearly with the jet power. These results strengthen and extend the validity of the results obtained by Allen et al. (2006) and Hardcastle et al. (2007), indicating that hot gas accretion is the dominant process in powering FR I radio galaxies across their full range of radio-luminosity. CoreG follow the same relationship, scaled to correspondingly lower accretion power.

This result, combined with the analogy of the nuclear properties, lead Balmaverde & Capetti (2006) to the conclusion that CoreG can be effectively considered as miniature radio galaxies. The exploration of the properties of these sources offers the opportunity to probe the physical properties of RLAGN at widely different levels of activity with respect to classical FR I radio galaxies. The aim of this paper is to expand the study of Balmaverde & Capetti (2006) by including i) an optical spectroscopic characterization of CoreG (derived by measuring ratios of emission lines) and ii) a detailed analysis of their radio properties (considering both morphologies and spectra), in order to perform a comparison with radio galaxies of higher power.

⋆ Based on observations made with the Italian Telescopio Nazionale Galileo operated on the island of La Palma by the Centro Galileo Galilei of INAF (Istituto Nazionale di Astrofisica) at the Spanish Observatorio del Roque del los Muchachos of the Instituto de Astrofisica de Canarias.

Table 1. Radio properties of the core galaxies.

Name	$F_{\rm core}$ mJy	$F_{74\ \rm MHz}$ mJy	$F_{1.4\ \rm GHz}$ mJy	$F_{5\ \rm GHz}$ mJy	$P_{\rm c}$	radio structure
UGC 5902	0.73[a]		2.4	0.7	0.30	VLA unresolved[e]
UGC 7203	4.8[b]		5.6	4.5	0.86	VLBI unresolved[m]
UGC 7629	4.8[a]		256	95	0.02	twin kpc jets[j]
UGC 7760	131.7[b]		100	121	1.30	twin pc jets[e]
UGC 7898	12.5[a]	449	29.1	24	0.43	twin kpc jets[k]
UGC 8745	10.5[a]	470	78.4	20	0.13	twin kpc jets[l]
UGC 9655	1.2[a]		14.8	2.1	0.08	VLA unresolved[h]
UGC 0968	1.5[c]		3.1	1.4	0.48	VLBI unresolved[i]
UGC 6297	2.7[a]		6.9	2.6	0.39	VLA unresolved[h]
UGC 7386	159.8[b]	343	385	351	0.41	pc jet[f,g]
UGC 7797	20.4[a]		36.8	21	0.55	twin pc jets[h]
UGC 7878	5.3[a]	692	77.8	45	0.07	twin kpc jets[k]
UGC 9706	6.4[d]		21.0	5.3	0.30	pc jet[i]
UGC 9723	12.7[b]		21.8	7.4	0.58	VLBI unresolved[n]

Column description: (1) name; (2) core flux at 5 GHz in mJy. References: (a) Baldi et al. 2009, in preparation; (b) Nagar et al. (2001); (c) Nagar et al. (2005) (VLBA); (d) Filho et al. (2004) at 8 GHz; ; (3) total flux at 74 MHz in mJy; (4) total flux at 1.4 GHz from Condon et al. (2002) in mJy; (5) total flux at 5 GHz from Wrobel & Heeschen (1991) and Wrobel (1991) in mJy; (6) core dominance, (7) radio morphology. References: (e) Nagar et al. (2002); (f) Jones et al. (1984); (g) Falcke et al. (2000); (h) Nagar et al. (2005); (i) Filho et al. (2004); (j) Ho & Ulvestad (2001); (k) Stanger & Warwick (1986); (l) Hummel et al. (1984); (m) Anderson et al. (2004); (n) Anderson & Ulvestad (2005).

The main finding of this study is that while from the nuclear point of view CoreG are simply scaled down version of FR I they have a deficit of a factor of ∼100 in extended radio emission with respect to that of classical FR I. We will show that, rather surprisingly, this is a general property, not limited to these faint radio sources, and that the vast majority of the population of RLAGN does not show the characteristic very luminous extended radio structures.

The paper is organized as follows. In Sect. 2 we present the sample selection. In Sects. 3 and 4 we analyze the radio and optical spectroscopic properties of the CoreG. This leads to a multiwavelength view of their nuclei (Sect. 5) that is compared with those of the more powerful 3CR/FR I. What emerges is that CoreG have a substantial deficit of extended radio emission. In Sect. 6 we show, considering different samples of radio sources, that radio galaxies with feeble extended structures represent the bulk of radio-loud AGN population. In Sect. 7 we discuss the consequences of this result on the general properties of radio galaxies and on our understanding of their nuclear activity. In Sect. 8 we summarize our findings and present our conclusions. In two Appendices we describe the details of the optical spectroscopic observations and explore the multiphase interstellar medium of CoreG.

2. Sample selection

Capetti & Balmaverde (2005) considered two samples (located in the Northern and Southern hemispheres) of luminous ($B \leq 14$), nearby ($V_{\rm rec} < 3000$) early-type galaxies for which extensive multiwavelength data from VLA, HST, and Chandra observations are available. They selected the galaxies detected in the VLA surveys of Wrobel & Heeschen (1991) and Sadler et al. (1989) at a flux limit of ∼1 mJy at 5 GHz, and used archival HST observations to study their surface brightness profiles. Balmaverde & Capetti (2006) focused on the 29 "core" galaxies, characterized by an flat inner logarithmic slope ($\gamma \leqslant 0.3$). As discussed in the Introduction they represent miniature versions of radio galaxies.

We extracted the Northern part of this sample of core galaxies (17 objects) for our observing programs, by leaving aside only the 3 powerful radio galaxies part of the 3CR sample, namely UGC 7360 (3C 270), UGC 7494 (3C 272.1, M 84), and UGC 7654 (3C 274, M 87). The final sample consists of 14 objects.

3. Radio properties of core galaxies

In order to analyze the radio properties of the CoreG, we first search in the literature for their radio maps, looking for extended emission. Twin jets are seen in the VLA images of UGC 7629, UGC 7878, UGC 7898, and UGC 8745 (the object descriptions with relative references and measured fluxes are given in Table 2), while all other sources are unresolved. Nonetheless, higher resolution data obtained with the VLBA (Nagar et al. 2005) detected sub-parsec scale jets for UGC 7386, UGC 7760, UGC 7797, UGC 9706. UGC 968, UGC 7203, and UGC 9723 are still unresolved even on the VLBA scale. No information on the parsec scale is available for UGC 5902, UGC 6297, and UGC 9655.

In general, the extended radio emission of these sources is dominated by the presence of jets, similar in morphology to those seen in FR I galaxies, but on smaller scales. The CoreG found to be extended in VLA images have sizes of 11–22 kpc, to be compared with the FR I part of 3C catalogue (see Chiaberge et al. 1999) whose sizes range from 8 to 400 kpc with a median of 100 kpc.

Using the total 1.4 GHz ($L_{1.4}$) and the 5 GHz core fluxes ($P_{\rm core}$) derived for several objects from our own A array VLA observations at 5 GHz (Baldi et al. 2009 in preparation), see Table 1, we estimated the core dominance of the sources of the sample, i.e. $P_{\rm c} = P_{\rm core}/L_{1.4}$. Most objects have a very high core dominance (Log $P_{\rm c} = -1$ and 0) compared to that measured in 3C/FR I objects (see Fig. 1). Three of the four objects with large scale jets (UGC 7629, UGC 7878, and UGC 8745) have, together with UGC 9655, the lowest core dominance, reaching the tail of the high core dominance of FR I.

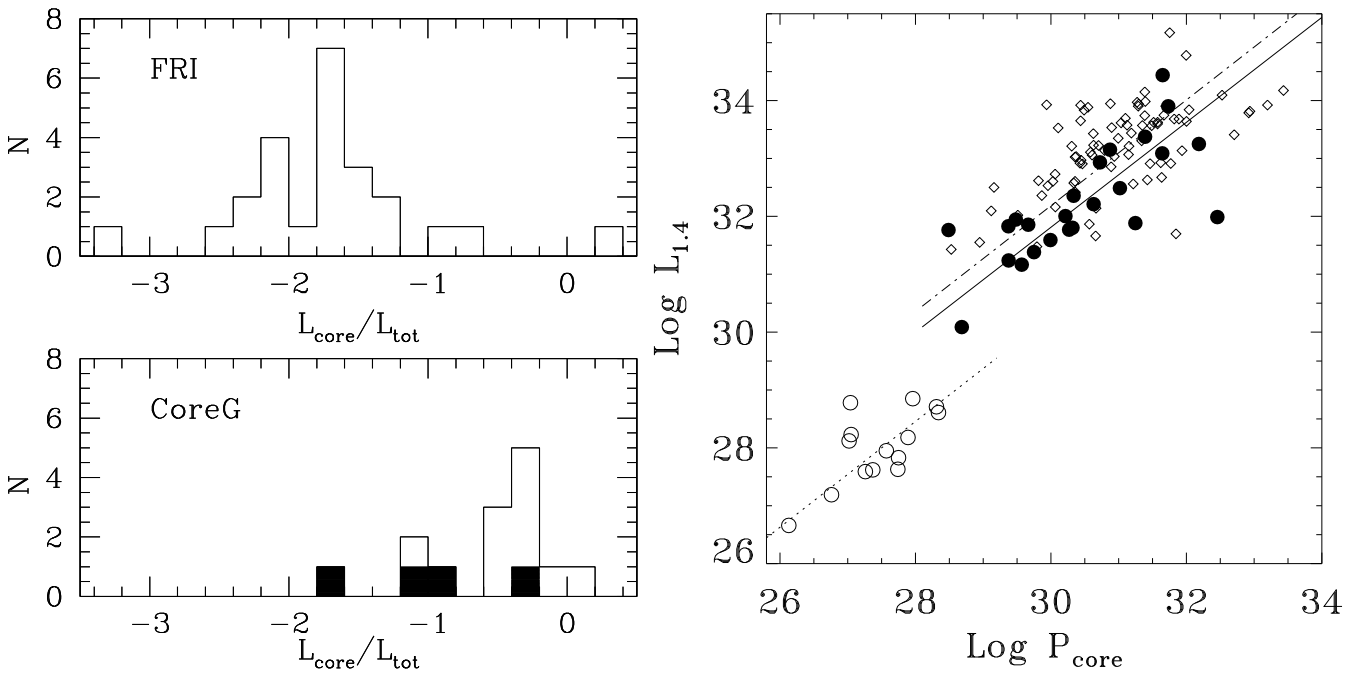

Fig. 1. *Left*: histograms of core dominance $P_c = P_{core}/L_{1.4}$ for the 3C/FR I and CoreG samples. *Right*: core radio power at 5 GHz vs. total emission at 1.4 GHz for CoreG (empty circles), 3CR radio galaxies (diamonds) where those with FR I morphology are indicated as filled circles. Lines indicate the best linear fit between the two quantities considered, dotted for CoreG, dot-dashed for 3CR, solid for 3CR/FR I.

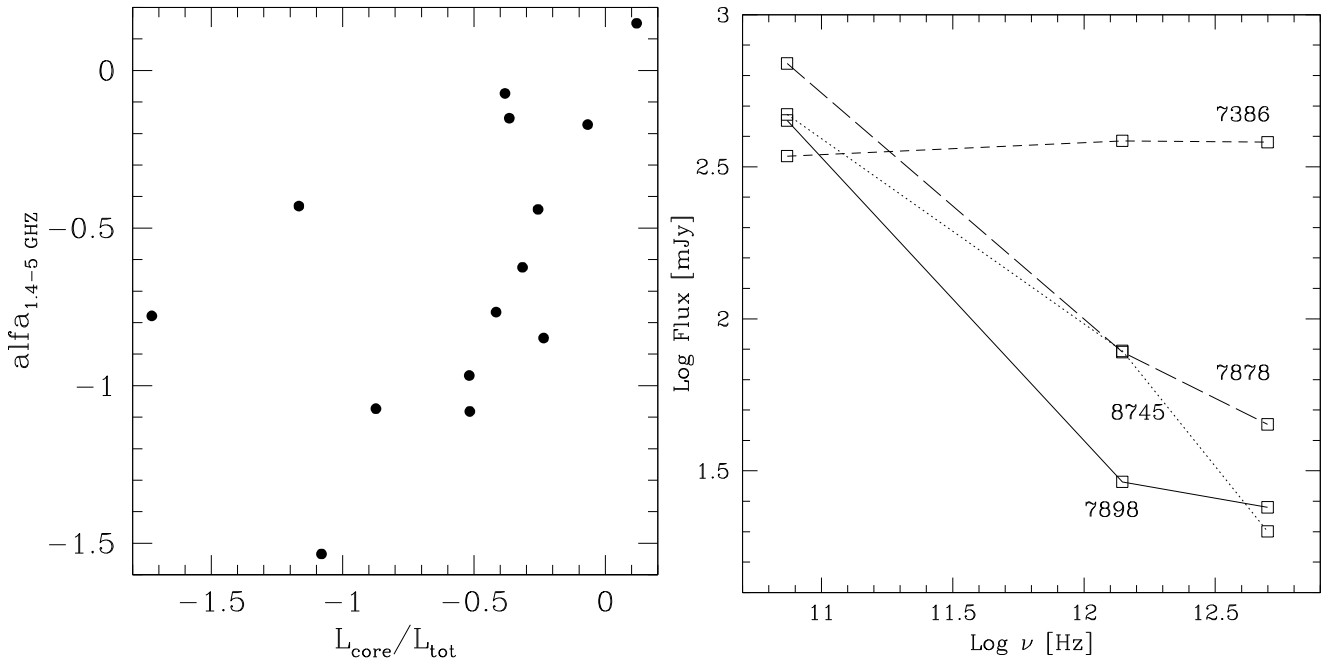

Fig. 2. *Left*: core dominance vs. spectral index between 1.4 and 5 GHz for the CoreG sample. *Right*: 3-point radio spectra of the 4 CoreG detected by the VLSS at 74 MHz.

To explore in more detail the core dominance of CoreG we compare in the right panel of Fig. 1 their core and total radio luminosities with those of all 3CR radio galaxies up to a redshift of $z = 0.3$. The core dominance in CoreG is a factor of ~100 higher than measured for the 3CR sample, or a factor of ~40 considering only the sample of 3CR/FR I selected by Chiaberge et al. (1999)[1].

Let us now focus on the radio spectral properties of the CoreG. We calculated the spectral index for the total emission between 1.4 and 5 GHz. Not surprisingly, the spectral index has a strong dependence on the core dominance (Fig. 2, left panel). Objects in which the flat spectrum core emission accounts for a

[1] From the original sample of Chiaberge et al. (1999) we excluded i) 3C 277.3, 3C 305, and 3C 433 since from an accurate inspection of its radio maps we revised its radio-morphological classification from FR I to FR II; ii) 3C 28, 3C 314.1, and 3C 348 because they belong to the spectroscopic class of Extremely Low Excitation Galaxies (ELEG) (Buttiglione et al. 2009b); iii) and 3C 386 because of the chance superimposition of a star on the galaxy's nucleus (Lynds 1971; Buttiglione et al. 2009a).

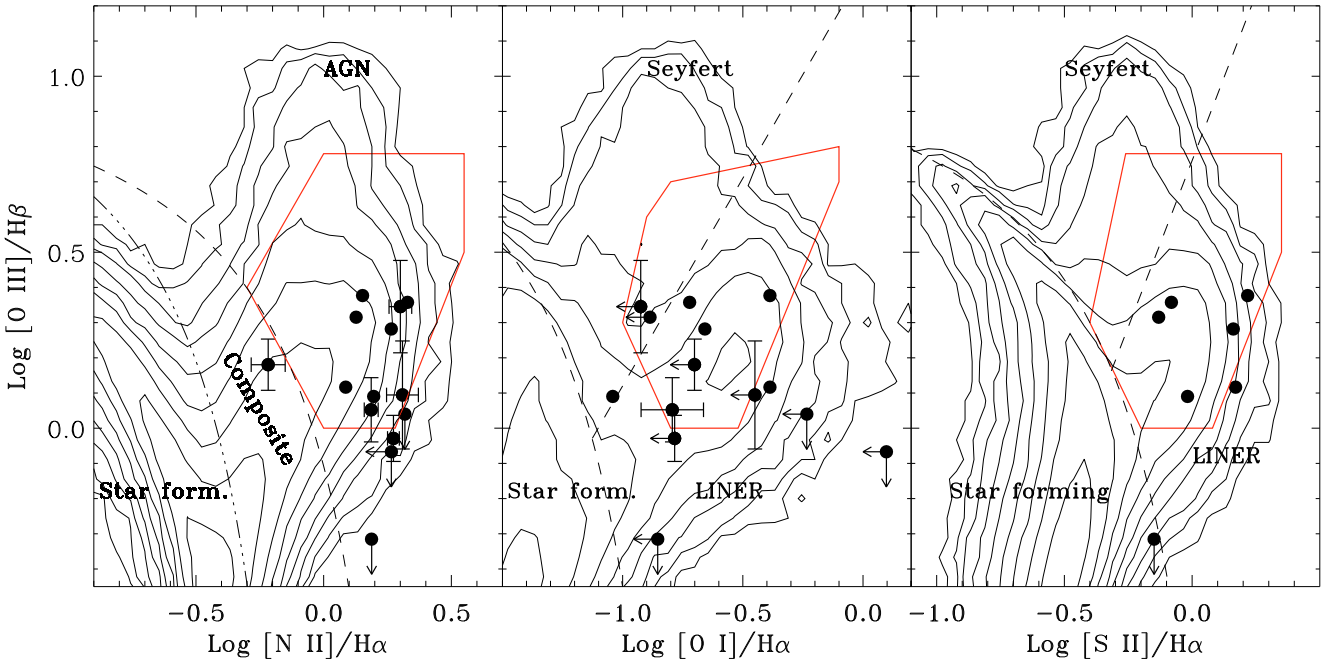

Fig. 3. Spectroscopic diagnostic diagrams: in *left panel*, log([O III]/Hβ) versus log([N II]/Hα), in *middle panel* log([O III]/Hβ) versus log([O I]/Hα), and in *right panel*, log([O III]/Hβ) versus log([S II]/Hα). The dashed separation lines among star forming galaxies, LINERs, and Seyferts is derived from Kewley et al. (2006), while the red box is the region covered by LEG in the 3CR sample (Buttiglione et al. 2009b). In the left panel the region between the dot-dashed and dashed lines is populated by composite galaxies, whose spectra contain significant contributions from both AGN and star formation.

large fraction of the total radio luminosity have lower spectral indices.

Four objects have been detected by the VLA Low-frequency Sky Survey at 74 MHZ (Cohen et al. 2007), namely UGC 7898, UGC07878, UGC 8745, and UGC 7386 (at a flux exceeding the 3σ limit of 0.3 Jy) and for these sources it is possible to build a three-point radio spectrum (see Fig. 2, right panel). The first 3 have rather steep spectra, with $\alpha_{74,1400} \sim 0.6$–$0.9$. These values are well within the range of the low frequency radio spectral indices measured by Kellermann et al. (1969) for the 3CRR radio galaxies, $\alpha_{38,750} \sim 0.75 \pm -0.15$. In UGC 7898 the spectrum is clearly convex, indicative of a transition from an optically thick (core) emission to the optically thin contribution of the extended structure at low frequencies. Instead, UGC 7386 still has a flat spectral index (–0.04), symptomatic of an extreme core dominance even at 74 MHz.

Therefore, although CoreG often show extended emission, often in the form of well defined jets, it is less extended and less dominant (with respect to the nuclear radio component) than in powerful radio sources. This effect cannot be ascribed in general to a different spectral behavior of CoreG with respect to FR I, as they show similar low frequency spectral indices. However, we cannot distinguish between the two alternative explanations for these results, namely that they are caused by Doppler boosting of the radio core or by a genuine deficit of extended radio emission.

4. Spectroscopic properties of core galaxies

The spectroscopic diagnostic diagrams, planes formed by pairs of emission line ratios, can be used to assess the nature of the nuclear emission, e.g. separating active nuclei from star forming galaxies (e.g. Baldwin et al. 1981). More recently, Kewley et al. (2006) selected a sample of ∼85 000 emission line galaxies from the SDSS, finding that Seyferts and LINERs (Heckman 1980) form separate branches in the diagnostic diagrams.

The spectroscopic survey of Ho et al. (1997) covers 13 out of 14 of the selected CoreG. However, the spectra of several galaxies are of insufficient quality to extract accurate line measurements and to obtain a robust spectral classification. We then re-observed 7 of these sources at the Telescopio Nazionale Galileo (TNG). The details of the observations are given in Appendix A. We obtained data at a resolution of $R \sim 800$ over the spectral range of 4650-6800 Å and extracted the spectra over a $2'' \times 2''$ nuclear region. We subtracted the contribution of the stellar emission using as a template two off-nuclear regions, $2''$ wide, flanking the nuclear aperture.

In all galaxies we were able to detect the Hα, Hβ, and [N II] lines and with only two exception (UGC 7898, and UGC 9655) we also measured the [O III] line. Conversely, only one spectrum (UGC 7203) yields an estimate of [O I]. In Table A.1 we report the line measurements for these 7 objects as well as those presented by Ho et al. (1997) for the remainder of the sample.

In general, the objects of our sample occupy a region in the first diagnostic diagram (see Fig. 3) indicative of an AGN origin of their emission lines. There are however a few possible exceptions: UGC 7898 only has measurements for the Hα line, but the limits of the diagnostic ratios are consistent with it being an AGN. Furthermore, UGC 5902 falls, in the first diagram, in the region of composite galaxies defined by Kewley et al. (2006), possibly the location of objects intermediate between star-bursts and AGN.

The second and third diagrams are less well defined, due to the smaller number of detections. In particular, since the wavelength coverage of our spectra does not include the [S II] lines, it is possible to include in the diagnostic diagram of log([O III]/Hβ) vs. log([S II]/Hα) only the 7 sources from Ho et al. (1997). Nonetheless, the location of the points is generally closely consistent with the region of LINERs according to the classification of Kewley et al. (2006).

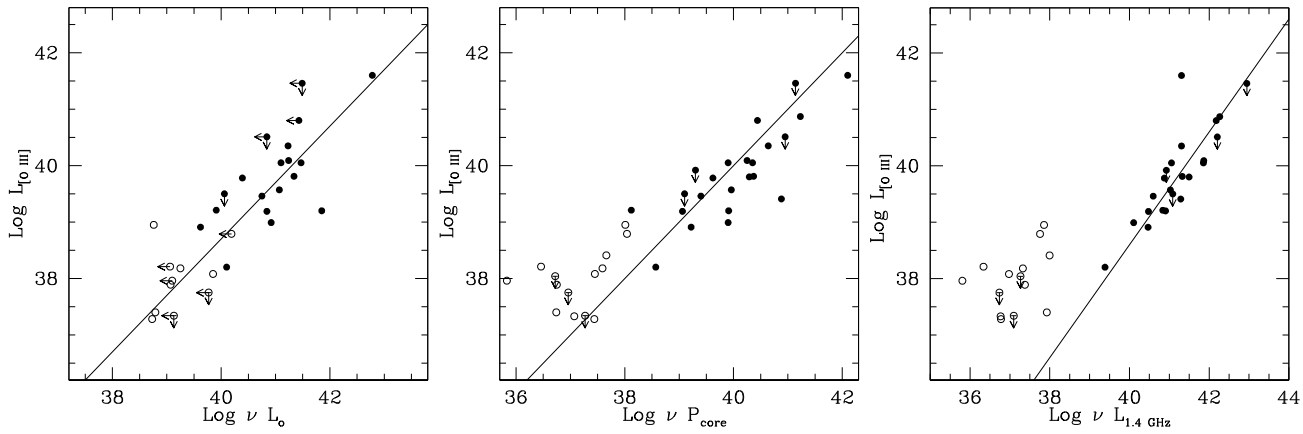

Fig. 4. [O III] line luminosity [erg s^{-1}] compared to the luminosities of (*left*) optical nucleus, (*center*) radio nucleus, and (*right*) total radio power at 1.4 GHz for Core galaxies (empty points) and 3CR/FR I (filled points). The solid lines are parallel to the planes bisectrix and mark the loci of constant ratio between the two quantities.

However, the AGN considered by Kewley et al. (2006) are mostly radio-quiet, while CoreG are radio-loud. Therefore, it is also instructive to perform a comparison with the results of Buttiglione et al. (2009b) on the spectroscopic properties of radio galaxies from the 3CR sample. Following previous studies, (e.g. Hine & Longair 1979; Laing et al. 1994; Jackson & Rawlings 1997), they separated low and high excitation galaxies (LEG and HEG respectively) on the basis of the narrow emission line ratios. In particular, the location of LEG in the diagnostic diagrams is represented by the red polygon in Fig. 3. Most of the CoreG are included in this area, generally populating its lower half, but also extending toward lower [O III]/Hβ ratios.

Buttiglione et al. (2009b) found that the separation between HEG and LEG respectively is similar to that found by Kewley et al. (2006) for LINERs and Seyferts among the SDSS sources. However, they found a significant number of LEG located above the line marking the transition between LINERs and Seyferts. The location of LEG shows an upward scatter with respect to the 'finger' of highest LINER density by ∼0.2 dex in the [O III]/Hβ ratio. Their data were not sufficient to conclude whether this was due to a genuine difference between the (mostly) radio-quiet AGN of the SDSS and the RLAGN of the 3CR sample, or simply to a luminosity difference. In fact, there is a substantial mismatch in luminosity between the 3CR and the SDSS sources, the former being brighter on average by a factor of ∼30.

The miniature radio galaxies considered here are instead well matched with the SDSS AGN. The majority of LINERs has luminosities in the range $10^{38} < L_{[O\ III]} < 10^{39}$ erg s^{-1}, while the sample of miniature radio galaxies discussed here has a median luminosity of $L_{[O\ III]} \sim 10^{38.3}$ erg s^{-1}. Indeed there is a close overlap between the two classes in the spectroscopic diagnostic diagrams. This indicates that the line ratios are driven mostly by the luminosity of the AGN rather than by its radio-loudness.

The main result derived from this analysis is that the observed line emission generally has an AGN origin, and it is not associated with star formation. This enables us to include the emission line luminosities in our analysis of AGN properties.

5. A multi-wavelength view of core galaxies

We collect multi-wavelength information for our sample of core galaxies in order to compare the emission in the different bands and to contrast it with the properties of the more powerful FR I radio galaxies. All data used for this analysis are reported in Table 2.

Table 2. Multiwavelength properties of the core galaxies.

Name	L_o	P_{core}	$L_{1.4\ GHz}$	$L_{[O\ III]}$
UGC 5902	<39.10	35.83	35.81	37.96
UGC 7203	39.85	37.45	36.98	38.08
UGC 7629	38.79	36.74	37.93	37.40
UGC 7760	38.73	37.44	36.78	37.28
UGC 7898	<39.13	37.27	37.10	<37.34
UGC 8745	–	37.66	38.00	38.41
UGC 9655	–	36.72	37.27	<38.04
UGC 0968	<39.77	36.96	36.74	<37.75
UGC 6297	<39.06	36.46	36.34	38.21
UGC 7386	38.76	38.01	37.86	38.95
UGC 7797	<40.19	38.04	37.76	38.79
UGC 7878	39.07	36.75	37.38	37.89
UGC 9706	39.25	37.59	37.33	38.18
UGC 9723	–	37.07	36.77	37.33

Column description: (1) name; (2) optical nuclear luminosity [erg s^{-1}] from Balmaverde & Capetti (2006); (3) radio core power [erg s^{-1}] at 5 GHz and (4) total radio luminosity at 1.4 GHz [erg s^{-1}] estimated from the fluxes given in Tab. 2; (5) [O III] emission line luminosity [erg s^{-1}].

As discussed, Balmaverde & Capetti (2006) found that the optical and X-ray nuclear luminosities correlate with the radio-core power, smoothly extending the analogous correlations already found for 3CR/FR I radio galaxies (Chiaberge et al. 1999; Hardcastle & Worrall 2000; Balmaverde & Capetti 2006) toward even lower power, by a factor of ∼1000, covering a combined range of 6 orders of magnitude. Apparently CoreG are simply scaled down version of 3CR/FR I from the point of view of their nuclear emission. This consideration also applies to the level of accretion of hot gas estimated by Balmaverde et al. (2008) in a sample of radio galaxies that includes both CoreG and 3CR/FR I. From the spectroscopic observations we also estimated that the warm ionized gas represents a small fraction (10^{-4}–7×10^{-3}) of the hot gas component (see Appendix B). This strengthens a posteriori the validity of the estimates of accretion rates derived considering only the high temperature gas.

The spectroscopic analysis of the CoreG rules out the star formation origin of the nuclear line emission. Therefore we can include the emission line luminosities in our analysis of the AGN properties. In Fig. 4 we show the [O III] emission line luminosities of the miniature radio galaxies with respect to the power of

their radio core, optical nucleus, and total radio emission. As a comparison, we also present the same quantities for the sample of 3CR/FR I radio galaxies, using the line luminosities measured by Buttiglione et al. (2009a).

The radio and the optical nuclear luminosities are well correlated with the emission line luminosities for both CoreG and 3CR/FR I, with CoreG extending these trends toward luminosities up to ∼100 lower with respect to 3CR/FR I radio galaxies. Conversely CoreG do not follow the relationship between total radio power and emission line defined by 3CR/FR I, showing an excess in line or a deficit in radio emission typically by a factor of ∼100.

In Sect. 3 we found a ratio between total and core radio emission approximately two orders of magnitude lower in CoreG than in 3CR/FR I radio galaxies. From the radio data alone the possibility that this is due to a Doppler boosting enhancement of the radio core emission remains viable. However, the inclusion of the emission line (a quantity independent of orientation) leads us to the conclusion that what we are seeing in CoreG is a genuine deficit of extended radio emission with respect to all estimators of nuclear activity compared to 3CR/FR I.

It must also be stressed that we always performed comparisons based on the total radio luminosity. For many CoreG, particularly those with the highest core dominance, the emission in the radio band is dominated by the radio core even at low frequencies, see for example the case of UGC 7386. Therefore, the derived deficits of extended radio emission should be considered as lower limits.

6. Revealing the bulk of the radio-loud AGN population

There are several possible alternatives to account for the different fractional level of extended radio emission with respect to the radio core observed in CoreG.

The first relies on the fact that CoreG have fainter radio cores than FR I. It can be envisaged that the ability of a RLAGN to produce a large scale jet is suddenly reduced below a critical nuclear luminosity, as suggested by the sharp drop in $L_{1.4}$ occurring at $P_{\rm core} \sim 10^{28.5}$ erg s^{-1} Hz^{-1} (see Fig. 1, right panel).

To test this possibility we looked for highly nucleated radio sources of higher luminosity than the CoreG considered here. In the 3CR sample widely used here as a benchmark, there are only two such sources, namely 3C 084 and 3C 371. However, in both cases the high $P_{\rm c}$ values are most likely due to Doppler boosting, since these galaxies host a highly polarized and variable optical nucleus (Miller 1975; Martin et al. 1976), typical of BL Lac objects.

We then considered another well studied sample, formed by the B2 radio galaxies (see Fanti et al. 1987, for its definition). We selected the sources with the highest values of $P_{\rm c}$ from Giovannini et al. (1988) setting an arbitrary threshold at $P_{\rm c} \gtrsim 0.1$,[2] yielding 11 objects. B2 0648+27 was later resolved into a compact (∼1″) steep spectrum (CSS) double (Morganti et al. 2003), while B2 1144+35B is a Gigahertz Peaked Source (GPS, Torniainen et al. 2007) with a peculiar radio-morphology (Giovannini et al. 2007); these objects will not be further considered here. One of them (B2 1217+29) is instead already included in our CoreG sample (as UGC 7386). For the remaining 8 radio galaxies we give their multi-band luminosities in Table 3.

[2] The core dominance estimated from Giovannini et al. (1988) is referred to the total luminosity at 408 MHz. This different definition is irrelevant for our purpose to find highly core dominated sources.

Table 3. Properties of the B2 sample.

Name	$F_{1.4\ \rm GHz}$	$F_{\rm core}$	$F_{[\rm O\ III]}$	$P_{\rm c}$
B2 0055+30	30.93[a]	30.46	39.45[a]	0.34
B2 0222+36	30.60[b]	30.46	40.63[b]	0.72
B2 0722+30	29.93[c]	29.55	–	0.42
B2 1101+38	31.18[d]	31.04	40.54[c]	0.72
B2 1557+26	30.67[a]	30.06	39.64[d]	0.25
B2 1638+32	32.11[a]	31.38	40.59[d]	0.19
B2 1652+39A	31.53[d]	31.43	40.65[e]	0.79
B2 2116+26	30.03[d]	29.38	39.44[f]	0.22

Column description: (1) name; (2) total luminosity at 1.4 GHz in erg s^{-1} Hz^{-1}. Reference: (a) White & Becker (1992); (b) Condon et al. (1998); (c) Becker et al. (1995b); (d) Condon et al. (2002); (3) core luminosity at 5 GHz in erg s^{-1} Hz^{-1} from Giovannini et al. (1988); (4) nuclear [O III] luminosity in erg s^{-1}. Reference: (a) Ho et al. (1997); (b) Buttiglione et al. (2010); (c) [O III] equivalent width from Jansen et al. (2000) and λ5007 continuum from Marcha et al. (1996); (d) from SDSS spectrum; (e) from Ha + [N II] measurement of Marcha et al. (1996) adopting [O III]/(Hα + [N II]) ∼ 0.38 (Hα/[O III] = 1 and [N II]/Hα = 1.6) (Buttiglione et al. 2009b); (f) from Hα + [N II] image (Capetti et al. 2005) with emission line ratios specified above; (5) core dominance, $P_{\rm c} = P_{\rm core}/L_{1.4}$.

We compared the core and the total radio emission (Fig. 5, left panel). Their core luminosity extends over the range $10^{29.5-31.5}$ erg s^{-1} Hz^{-1}, three orders of magnitude higher than CoreG, while covering essentially the same range of the 3CR/FR I sample, and, by construction, lying close to the line of equal core and total luminosity.

From the point of view of line emission, they are located in the same region of the $L_{[\rm O\ III]}$ vs. $P_{\rm core}$ plane of the 3CR/FR I sources (Fig. 5, middle panel) following the same relationship. However, they have a deficit of total radio luminosity at a given line luminosity of an average factor of ∼30 (Fig. 5, right panel), a result similar to what was found by Morganti et al. (1992). As already mentioned above, this value should be considered as a lower limit in terms of *extended* radio emission vs line luminosity.

These B2 radio galaxies represent the high luminosity counterparts of CoreG from the point of view of their multi-wavelength properties, thus contrasting with the proposed scenario that only AGN of low core power produce sources with feeble extended radio emission.

The second possibility ascribes the presence of AGN with high and low $L_{[\rm O\ III]}/L_{\rm ext}$ ratios to the existence of two distinct populations. They could arise from, for example, a different mechanism of jet launching or of jet composition in the two classes. This predicts a bimodal distribution of core dominance within a given sample. Such an effect is not observed either in the B2 or in the 3CR samples (Feretti et al. 1984).

Our preferred interpretation is that, instead, the prevalence of low core dominance sources in low frequency flux limited samples is due to a selection bias. For example, a radio source is part of the 3CR when its total flux exceeds >9 Jy (Spinrad et al. 1985). The sole core flux of 3CR sources never reaches this threshold (with the only exception of 3C 084 with $F_{\rm core} \sim 42$ Jy). Thus, a significant contribution from the extended emission is required to be part of the 3CR, favoring AGN with low $L_{[\rm O\ III]}/L_{\rm ext}$ ratios. The lower flux threshold of the B2 (250 mJy at 408 MHz, Fanti et al. 1978) allows the inclusion of a larger fraction of core dominated galaxies. The higher frequency and the much lower flux limit (1 mJy at 5 GHz), imposed on our CoreG sample, drastically reduces the selection bias against sources with

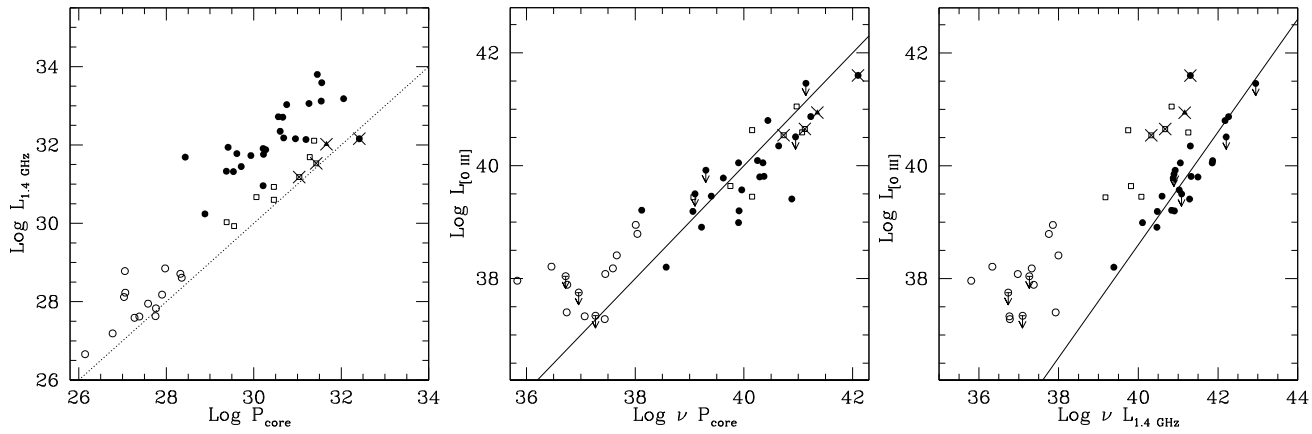

Fig. 5. Comparison of [O III] line, core, and total radio luminosities for CoreG (empty circles), 3CR/FR I (filled circles), and a sub-sample of high core dominance B2 radio galaxies (empty squares). The crossed symbols locate the BL Lac objects in the B2 (B2 1101+38 and B2 1652+39A) and 3CR samples (3C 371, marked with a triangle, and 3C 84). The lines represent a constant ratio between the two quantities; in the *left panel* the dotted line marks the locus of equal core and total radio emission.

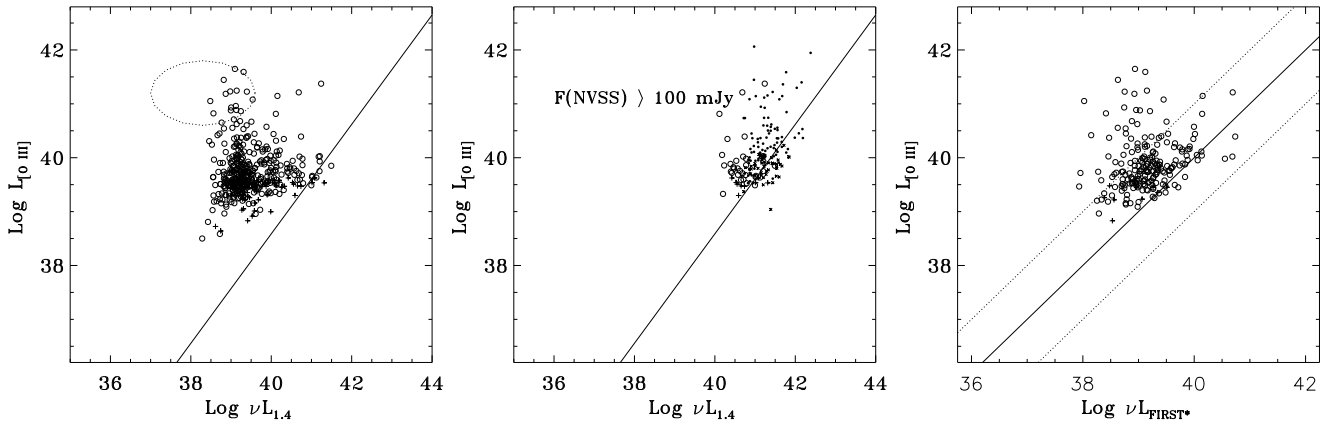

Fig. 6. *Left panel*: comparison of [O III] luminosity with total radio power for the SDSS/NVSS AGN sample (from Best et al. 2005b) with $0.03 < z < 0.1$. The plus symbols are upper limits in [O III]. The solid line marks the equal ratio between the two quantities normalized to the 3CR sources. The ellipse represents the location of Seyfert galaxies (Nagar et al. 1999) in this plane. *Middle panel*: same as the left panel but restricted to sources with $F_{1.4} > 100$ mJy, equivalent to the selection threshold of the B2 sample. Higher redshift sources ($0.1 < z < 0.3$) are also included as dots (or crosses for [O III] upper limits). *Right panel*: luminosity of the central component in the FIRST images, $L_{\mathrm{FIRST}*}$, as a proxy for the radio core (we considered only objects in which the size of this component is smaller than 3″), versus line luminosity. The dotted lines in the right panel indicate a change of the ratio by ±1 dex.

high $L_{[\mathrm{O\ III}]}/L_{\mathrm{ext}}$ ratios. As a result, the CoreG sample is formed predominantly by galaxies of high core dominance[3].

In order to test this scenario, we now include in the analysis the RLAGN selected by Best et al. (2005b) cross-matching the ∼212 000 galaxies drawn from the SDSS-DR2 with the NVSS and FIRST[4] radio surveys. Leaving aside 497 sources identified as star forming galaxies, this yields 2215 radio luminous AGN brighter than 5 mJy at 1.4 GHz. In Fig. 6 we show their location in the $L_{[\mathrm{O\ III}]}$ vs. $L_{1.4}$ plane limited to the 425 sources with $0.03 < z < 0.1$, for consistency with Best et al. (2005b). Most sources are located around $L_{[\mathrm{O\ III}]} \sim 10^{39.5}$ erg s^{-1}, while spanning a range in $L_{1.4}$ of 3 orders of magnitude, $L_{1.4} \sim 10^{38.5}$–$10^{41.5}$ erg s^{-1} Hz^{-1}. The behavior of higher redshift sources, up to $z = 0.3$, is similar but shifted at higher radio and [O III] power by ∼0.7 dex. The vast majority of the objects lie a factor of ∼100 to the left of the relationship between line and radio emission defined by the 3CR sources and, actually, the source density increases at lower $L_{[\mathrm{O\ III}]}/L_{1.4}$ ratios. The bulk of the population of this SDSS/NVSS AGN sample thus shows a large deficit of total radio emission, similar to that observed in CoreG.

For these sources there are no measurements of the radio core fluxes. A possible proxy for the radio core is the flux of the central component seen in the FIRST images, $F_{\mathrm{FIRST}*}$, tabulated by Best et al. (2005b). We considered only the 256 objects in which the size of this component is smaller than 3″, at most marginally resolved at the 5″ resolution of the survey. The comparison between $L_{[\mathrm{O\ III}]}$ and $L_{\mathrm{FIRST}*}$ is shown in Fig. 6. With the caveat that this is not a genuine measurement of the radio core, we note that the bulk of this sample has a ratio of the line with respect to the central radio component that is slightly larger, by a factor of ∼3, than those the 3CR and B2 samples discussed above, but similar to that measured in the lower luminosity CoreG[5].

[3] We remind that three nearby 3CR sources (UGC 7360 alias 3C 270, UGC 7494 alias 3C 272.1, and UGC 7654 alias 3C 274) are part of the initial CoreG sample.

[4] Sloan Digital Sky Survey, (York et al. 2000), National Radio Astronomy Observatory (NRAO) Very Large Array (VLA) Sky Survey (Condon et al. 1998), and the Faint Images of the Radio Sky at Twenty centimeters survey (Becker et al. 1995a) respectively.

[5] There are a minority of objects, ∼10% of the sample, forming a substantial tail toward high values of $L_{[\mathrm{O\ III}]}$, a point to which we will return in the next Section.

A simple exercise can prove the selection biases discussed above. From the NVSS/SDSS sample, we extracted the radio sources that would meet the radio selection criterion imposed on the B2 sample, i.e. $F_{408\ \mathrm{MHz}} > 250$ mJy, that translates into ∼100 mJy at the 1.4 GHz NVSS, frequency having adopted a radio spectral index of 0.7. The resulting sample, including sources up to $z = 0.3$, is shown in the right panel of Fig. 6. We selected only sources lying along the relation between $L_{1.4}$ and $L_{[\mathrm{O\ III}]}$ defined by the 3CR sources, while all sources with a deficit of total radio emission are discarded.

We conclude that when the selection biases used are less severe (lower flux threshold and/or higher frequency), core dominated radio galaxies emerge as the dominant constituent of the population of RLAGN. Conversely, the most studied catalogues of radio galaxies, selected at high fluxes and low frequencies, are composed of the minority of RLAGN that meet the physical conditions required to form extended radio sources.

7. Discussion

The results discussed in the previous sections indicate that in RLAGN all indicators of nuclear activity, i.e. line luminosity, power of the radio core, and (when available) the luminosity of the optical and X-ray nucleus, are all closely and quasi-linearly correlated to each other despite the fact that they cover a range of ∼6 orders of magnitude. This is evidence that from the point of view of the nuclear properties, the RLAGN population is very homogeneous.

Conversely, RLAGN present an extremely large range of total radio power, a factor of ∼1000, at a given level of radio core or emission line luminosity. The vast majority of the population is associated with sources of relatively low levels of extended radio emission with respect to classical FR I radio galaxies. Even the NVSS/SDSS sample is not completely free from selection biases and that the space density of core dominated sources might be even higher, and extending to more extreme ratios of core versus extended emission.

The most studied catalogues of radio galaxies are severely biased against the inclusion of objects with high core dominance, since a large contribution from extended emission is needed to fulfill the stringent flux requirements of low frequency, high flux threshold samples. They are thus composed of the minority of AGN that meets the physical conditions required to form extended radio sources, while the bulk of the RLAGN population is virtually unexplored.

It is important to stress that these AGN, despite the lower level of extended radio emission, are not radio-quiet. Not only do they have radio-loud nuclei, but they have (on average) a ratio between radio and line luminosity larger by a factor of 300 with respect to radio-quiet AGN of similar radio luminosity. This is clearly seen in Fig. 6, where we reproduce the location of the sample of Seyfert galaxies studied by Nagar et al. (1999).

From the point of view of the host galaxies of the core dominated radio galaxies, for the sample of Core galaxies they are massive early-type (E and S0) galaxies, less luminous than the 3CR/FR I host on average by 1 magnitude, but the luminosity ranges of the two classes overlap considerably (Balmaverde & Capetti 2006). Their black hole masses are $10^{7.8-9.5}\ M_\odot$, with a distribution indistinguishable from those measured in 3CR/FR I hosts. The SDSS/NVSS sample of Best et al. (2005b) is also formed predominantly by massive objects ($M \sim 10^{10-12}\ M_\odot$, with an average of $\sim 10^{11.5}\ M_\odot$) and with black hole mass in the range $10^{6.8-9.5}\ M_\odot$ (average value of $\sim 10^{8.5}\ M_\odot$), similar to those of 3CR/FR I. A detailed study of the morphology and colors of the SDSS/NVSS hosts will be the subject of a forthcoming paper, but, apparently, high and low core dominance radio sources cannot be readily separated on the basis of differences in their hosts.

The environment could also play an important role. Analyzing the literature, we found that CoreG typically are the brightest galaxies of groups of intermediate richness. With respect to 3C/FRI they seem to avoid the center of rich clusters. Instead, at the moment there are no indications in the environment of the bulk of the SDSS/NVSS radio-loud AGN population.

One possibility to account for the sequence from low to high extended power, at the same level of nuclear activity, is to assume a relation with the source age, in the sense that low power sources are younger that those of higher power. This requires that the radio luminosity increases with time as the radio source expands. Furthermore, the growth of the radio luminosity must depend strongly on age to reproduce the relatively higher density of sources with the lowest radio power. This requirement contrasts with what is derived for the luminosity evolution of CSS and GPS sources (see e.g. Snellen et al. 2000), a general result based on self-similarity and on the formation of pressured confined radio-lobes. Nonetheless, lower power sources might form predominantly plume-like radio structures and all is further complicated by the possibility of recurrent outflows, slowly burrowing their way into the interstellar medium of the host galaxy.

In a similar line of interpretation, the high number of young/faint sources is expected if they are short lived and they never grow to large scales. Alexander (2000) presented an analytical model for the evolution of radio sources from small physical scales to classical doubles; they found that observational data can be reproduced assuming the presence of a population of sources that suffer disruption of their jets before escaping the host core radius. This scenario confirms earlier predictions that compact symmetric objects (CSOs), with typical sizes of ∼100, could switch off after a short period of time, ∼3000 years, possibly due to a lack of sufficient fueling (Readhead et al. 1994; Kunert-Bajraszewska & Thomasson 2009). Similarly, Reynolds (1997) proposed a model in which radio sources are intermittent on timescales of $\sim 10^4$–10^5 years. If this is the correct interpretation, the question is why classical FR I are active over large timescales, necessary to form radio structures up to the Mpc scale, while the majority of the RLAGN population is short lived.

The very large range of total radio-power at a given level of emission line luminosity lead Best et al. (2005a) to argue that they are independent phenomena, triggered by different physical mechanisms. Indeed our results point to the conclusion that the total radio emission is not simply determined by the AGN activity level. Conversely, the radio-core luminosity, despite the effects of beaming, is closely linked to line emission and it is a rather good indicator of nuclear activity. Capetti et al. (2005) argued that the strong correlation between line and optical continuum nuclear emission found for 3CR/FR I radio galaxies suggests that the optical cores (most likely of non-thermal origin) can be directly associated with the source of ionizing photons, i.e. that we are seeing a jet-ionized narrow line region. This suggests that the primary link between radio core and line luminosity is due to the relationship existing between both quantities with the optical core. Conversely, the well established correlation between total radio and line luminosities (e.g. Baum & Heckman 1989; Rawlings et al. 1989; Rawlings & Saunders 1991) is likely to be the result of the selection of radio sources

of similar range of core dominance, imposed by the selection criteria of the sample.

The indication that the bulk of the RLAGN population is not represented in the well studied samples of radio galaxies also requires us to revise profoundly the unified models based on orientation for the low luminosity RLAGN (see e.g. Urry & Padovani 1995). The behavior of the two 3CR sources with the highest core dominance (3C 084 and 3C 371) is very instructive in this context. They show an excess of the radio core with respect to the sources of similar $L_{[\mathrm{O\ III}]}$, as expected considering the Doppler boosting of their nuclear emission. Nonetheless, they have a strong deficit in total radio emission, given their [O III] luminosity, despite the enhanced core contribution. The same result applies to the two well known BL Lac objects that is part of the B2 sample (B2 1101+38 alias MRK 421 and B2 1652+39A alias MRK 501). The beaming effects favor their inclusion in the flux limited samples but these sources, if they were observed along a line of sight forming a larger angle with the jet axis, would show an even larger offset from the relationship between radio and line luminosity defined by the 3CR sample. The small number statistics suggests some caution, but this supports the idea that the parent population of BL Lac sources, and thus the overall population of radio galaxies, is dominated by sources with high $L_{[\mathrm{O\ III}]}/L_{\mathrm{ext}}$ ratios. Furthermore, our results indicate that a high core dominance in a radio source cannot be taken as sole evidence to deduce a strong Doppler boosting, in line with the suggestion of Marchã et al. (2005).

The vast population of core dominated radio galaxies might also have consequences on the predictions and interpretation of the density of high radio frequency extragalactic sources (see e.g. de Zotti et al. 2005) relevant for the experiments on the Cosmic Microwave Background, and also on the association between AGN and the high energy cosmic rays (see e.g. Abraham et al. 2007).

We conclude this section considering the minority of objects in the SDSS/NVSS sample form a substantial tail toward high values of $L_{[\mathrm{O\ III}]}$ with respect to the power of the central FIRST component (see Fig. 6, right panel), our proxy for the core power. These sources are located in the region where radio-quiet AGN are found (see Capetti & Balmaverde 2006; Capetti et al. 2007), being characterized by larger $L_{[\mathrm{O\ III}]}/P_{\mathrm{core}}$ ratios than radio loud AGN. They have radio luminosities $L_{1.4} \sim 10^{29.5-31}$ erg s^{-1} Hz^{-1}, well within the range of Seyfert galaxies (Ulvestad & Wilson 1984), suggesting a possible contamination of the SDSS/NVSS sample by radio-quiet AGN. Clearly these objects deserve further study, particularly concerning their optical spectroscopic classification and their radio structure, aimed to accurate radio core measurements.

8. Summary and conclusions

We considered a sample of 14 luminous and nearby early-type galaxies hosting miniature RLAGN of extremely low radio luminosity (10^{27-29} erg s^{-1} Hz^{-1} at 1.4 GHz) for which an extensive radio and optical analysis is performed. We collect the multiwavelength nuclear information for our sample of core galaxies in order to compare them with those of the more powerful FR I radio galaxies.

A radio analysis of these sources reveals that in many CoreG, the extended radio morphology is indicative of a collimated outflow. However, they are substantially less extended (up to ~20 kpc) and their core dominance is a factor of 40–100 higher than in more powerful FR I radio sources in the 3CR sample. Their radio spectral properties are instead similar to those of 3CR/FR I.

We also obtained new optical spectroscopic observations. CoreG show emission line ratios typical of AGN (they can be classified as low excitation galaxies), similar to, but of even lower excitation than, those of 3CR/FR I radio galaxies, and matching more closely those of radio-quiet AGN of the same of line luminosity. This indicates that the line ratios are driven mostly by the AGN luminosity rather than by its radio-loudness.

The main result obtained from the spectroscopic study is that the observed line emission has generally an AGN origin and this enables us to include these emission lines in our analysis of the AGN properties. While miniature radio galaxies follow similar relationships to those found for more powerful radio galaxies in terms of line, optical, and radio nuclear luminosities, as well as accretion rate, they have a deficit of a factor of ~100 in extended radio emission with respect to that of classical 3CR/FR I. From the radio data alone, the possibility that this is due to a Doppler boosting enhancement of the radio core emission was still viable. The inclusion of emission lines (independent of orientation) leads us to conclude that what we are seeing in CoreG is a genuine deficit of extended radio emission, considering different estimators of nuclear activity, with respect to 3CR/FR I.

The deficit of extended radio emission is also found in radio sources extracted from the B2 sample, with radio cores as powerful as those of classical FR I radio galaxies. Therefore, the difficulty to produce prominent extended radio structures is not simply due to a low AGN luminosity. Actually, core dominated sources form the bulk of radio-loud AGN population in the SDSS/NVSS sample. The vast majority of these sources show, at a given level of line luminosity, a deficit of radio emission of a factor of ~100. Furthermore, this value should be considered as an upper limit due to the significant contribution of the radio core and since the samples considered are not completely free from selection biases.

At a given level of nuclear emission, one can find radio sources with an extremely wide range of radio power. Nonetheless, even the objects with the lowest level of extended radio emission are not radio-quiet. Not only are their nuclei radio-loud, but they have on average a ratio of radio to line luminosity larger by a factor of 300 with respect to radio-quiet AGN of similar radio power.

One possibility to explain this effect is to assume that this is driven by the source age, assuming that the radio luminosity increases with time as the radio source expands. A high number of young/faint sources is expected if the vast majority of RLAGN is short lived and never grows to large scales. If this is the correct interpretation, the questions are: what mechanism sets the lifetime of the radio galaxies? Why are most radio-loud galaxies short-lived, while only a minority is active over long timescales?

The prevalence of low core dominance sources in flux-limited samples is apparently due to a selection bias, since the inclusion of sources with luminous extended radio structures is highly favored. This result has several important ramifications. For example, unified models for RLAGN should be at least in part reconsidered, since the bulk of the RLAGN population is not well represented in the most studied samples of radio galaxies. Similarly, the relationship between line and radio emission results at least in part from selection effects, while apparently the link between the line and radio core is more robust and relies on the common dependence of these quantities on the strength of the nuclear continuum emission.

A thorough study of the morphology and colors of the hosts of core dominated sources, in particular those that are part of

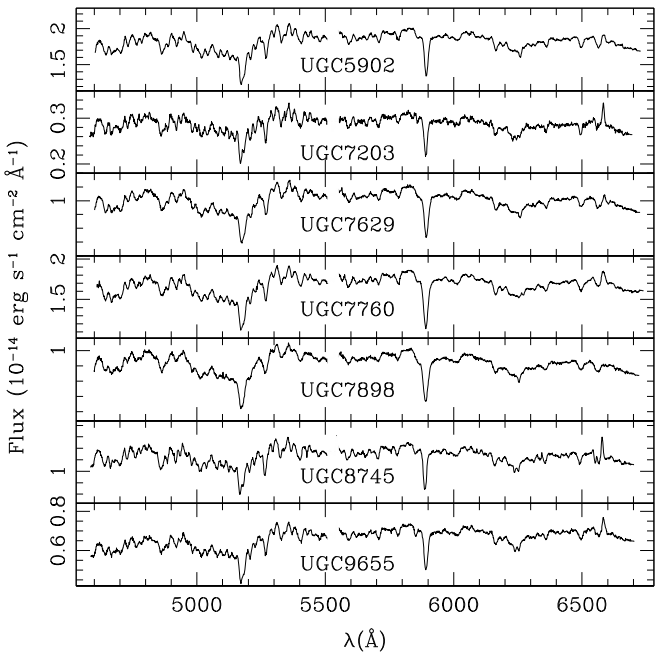

Fig. A.1. Spectra of the 7 sources observed at the TNG. The wavelength scale has been corrected for the redshift reported in Table 2. For each object the flux scale covers the range (0.6–1.2) × $F_{\lambda=5500}$.

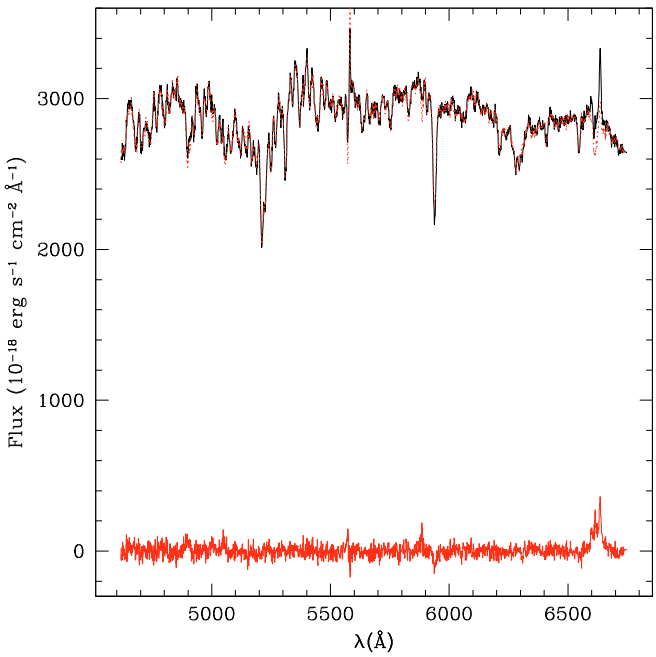

Fig. A.2. Spectrum of UGC 7203 as an example of the subtraction of galaxy emission (red dashed line) from the nuclear spectrum (black solid line). The residuals, shown on the bottom, provide the genuine spectrum of the AGN.

the large SDSS/NVSS sample, as well as of their radio morphology and optical spectroscopic classification is clearly required. This will enable us to perform a more detailed comparison with classical extended radio galaxies to reveal further similarities or differences that might account for their diversity.

The samples considered here are limited to AGN with $L_{[O\ III]} \lesssim 10^{41}$ erg s^{-1}. It would be of great interest to explore whether the dominance of radio galaxies with relatively low extended radio emission applies also to sources of higher power.

Appendix A: Spectroscopic observations of core galaxies

On 2006 10th March we observed a subsample of 7 CoreG with Telescopio Nazionale Galileo (TNG), a 3.58 m optical/infrared telescope located on the Roque de los Muchachos in La Palma, Canary Islands (Spain). We selected the sources for which the spectra available from the survey of Ho et al. (1997) are of insufficient quality to extract accurate line measurements and to obtain a robust spectral classification. The available spectrum of an additional galaxy, UGC 968, is also of rather poor quality, but was not visible during the observing run.

The observations were made using the DOLORES (Device Optimized for the LOw RESolution) spectrograph installed at the Nasmyth B focus of the telescope, with an exposure time of 1200 s. The chosen long-slit is 2″ wide. For each target we used the VHR-V grism which has a dispersion of 1.05 Å/pixel, a spectral coverage of 4650–6800 Å and a resolution of $R \sim 800$.

The spectra were reduced using the LONGSLIT package of IRAF[6]. The optical spectra were processed by the standard spectroscopic calibration (bias subtraction, flat field normalization, background subtraction, wavelength calibration, and flux calibration with spectrophotometric standard stars). We then summed and extracted a region of 2″ along the spatial direction, resulting in a region covered by our spectra of 2″× 2″.

The spectra obtained with this aperture contain emission from the active nucleus as well as a substantial contribution from the host galaxy stellar population. To proceed in our analysis it is necessary to separate these two components by subtracting the starlight from the extraction aperture.

In order to estimate the contribution of stellar emission, we used as a template the spectra extracted from two off-nuclear regions, 2″ wide, flanking the nuclear aperture. We then appropriately scaled the template to match the nuclear spectrum, by excluding from the match the spectral regions corresponding to emission lines, as well as other regions affected by telluric absorption, cosmic rays or other impurities. The subtraction of this stellar emission template from the nuclear aperture gives us the genuine nuclear emission spectrum. This method is illustrated in Fig. A.2, where we show an example of starlight subtraction. Note that, since the AGN optical core of these radio sources (Balmaverde & Capetti 2006) contributes to ≲1/100 of the light within the extraction region, we can neglect the presence of nuclear continuum emission in the spectra. The accuracy of the starlight subtraction can be assessed by the absence of large-scale patterns in the residual spectra at a typical amplitude of $<0.5 \times 10^{-16}$ erg s^{-1} cm^{-2} Å^{-1}. The noise rms is of $<10^{-16}$ erg s^{-1} cm^{-2} Å^{-1}.

The next step of our analysis consists of the measurement of the emission line intensities, for which we used the SPECFIT package in IRAF. We measured line intensities fitting Gaussian profiles to H$\beta\lambda$4861, [O III]$\lambda\lambda$4959,5007, [O I]$\lambda\lambda$6300,6364, H$\alpha\lambda$6563, [N II]$\lambda\lambda$6548,6584 (Table A.1). Some constraints were adopted to reduce the number of free parameters: we required the width5 and the velocity to be the same for all the lines. The integrated fluxes of each line were free to vary except for those with known ratios from atomic physics: i.e. the

[6] IRAF is the Image Reduction and Analysis Facility of the National Optical Astronomy Observatories, which are operated by AURA, Inc., under contract with the U.S. National Science Foundation. It is also available at http://iraf.noao.edu/.

Table A.1. Optical emission line fluxes of the core galaxies.

Name	V	Hβ	[O III]	[O I]	Hα	[N II]	[S II]
UGC 5902	950	3.2 ± 0.5	4.8 ± 0.4	<1.2	6.2 ± 0.7	3.8 ± 0.4	–
UGC 7203	2379	0.9 ± 0.1	1.0 ± 0.1	0.5 ± 0.1	2.8 ± 0.1	4.4 ± 0.2	–
UGC 7629	1047	0.9 ± 0.2	1.1 ± 0.2	<0.6	1.6 ± 0.2	3.3 ± 0.2	–
UGC 7760	450	2.0 ± 0.5	4.4 ± 0.7	<1.2	10 ± 1	20.0 ± 0.4	–
UGC 7898	1198	0.8 ± 0.2	<0.7	<0.8	0.6 ± 0.2	<1.2	–
UGC 8745	2054	3.0 ± 0.3	2.8 ± 0.3	<1.1	6.4 ± 0.3	12.0 ± 0.3	–
UGC 9655	2037	1.1 ± 0.3	<1.2	<0.91	1.6 ± 0.3	3.3 ± 0.3	–
UGC 0968	2422	0.94[b]	<0.45	<0.42	3.0	4.7	2.1
UGC 6297	1025	3.2	7.3	3.4	18	38	15
UGC 7386	788	51	67	54	132	161	195
UGC 7797	2283	2.4	5.6	4.6	11	16	19
UGC 7878	1012	1.9	3.6	1.2	5.4	9.9	7.8
UGC 9706	1832	1.7	2.1	0.6[c]	6.6	10	6.3
UGC 9723	950	0.54	1.1	<0.47	3.6	4.9	2.7

Column desctription: (1) name; (2) radial velocity (cz) corrected for Local Group infall onto Virgo cluster [km s^{-1}]; emission line flux in units of 10^{-15} erg s^{-1} cm^{-2}: (3) H$\beta\lambda$4861, (4) [O III]λ5007, (5) [O I]λ6300, (6) H$\alpha\lambda$6563, (7) [N II]λ6584, (8) sum of [S II]λ6716 and [S II]λ6731. The upper limit fluxes are measured at 3σ. The data below the horizontal line are from Ho et al. (1997). For these sources, values with uncertainties of ±30%–50% are marked by 'b', while highly uncertain values with probable errors of ±100% are marked by 'c'.

[O I]$\lambda\lambda$6300,64, [O III]$\lambda\lambda$4959,5007 and [N II]$\lambda\lambda$6548,84 doublets. After subtraction of the narrow line components we did not find significant residuals around the Balmer lines that might indicate the presence of a broad line region. In Table A.1 we report the line measurements for these 7 objects as well as those presented by Ho et al. (1997) for the remaining sample.

Appendix B: The multiphase inter-stellar medium of early-type galaxies

As discussed in the Introduction, the level of activity in CoreG and FR I is closely related to the accretion rate of hot gas, that represents the dominant process in powering these radio sources. The line emission detected in the sources of our sample can be used to estimate the amount of relatively cold ionized gas present in their nuclear regions, to be then compared with the hot ISM component.

Following Osterbrock (1989), in the case B approximation, we have:

$$M_{\rm H\,II} = \frac{m_{\rm p} + 0.1 m_{\rm He}}{n_{\rm e} \alpha^{\rm eff}_{\rm H\beta} h\nu_{\rm H\beta}} L_{\rm H\beta} \approx \frac{3 \times 10^{-36}}{n_3} L_{\rm H\alpha}\ M_\odot$$

where n_3 is the gas electronic density in 10^3 cm^{-3} units and we assumed a recombination coefficient of $\alpha^{\rm eff}_{\rm H\beta} = 3.03 \times 10^{-14}$ cm^3 s^{-1}, i.e. a temperature of 10^4 K, and $L_{\rm H\beta} = L_{\rm H\alpha}/3$. The resulting masses are in the range 40–1800 $M_\odot$.

On the other hand, we can use the results of Balmaverde et al. (2008) to estimate the mass of the X-ray emitting hot gas in the galactic coronae. From the brightness profiles of the Chandra images, they derived the gas density profiles that can be integrated out to the same physical radius $r_{\rm spec}$ used to extract the optical spectra,

$$M_{\rm hot} = 2\pi n_{\rm B} r_{\rm B}^3 \left(\frac{r_{\rm spec}}{r_{\rm B}}\right)^2$$

where $n_{\rm B}$ is the electronic density at the Bondi radius r_B, having used the averaged logarithmic slope ($\alpha \sim -1$) of the density profiles to perform the integration.

The masses of the hot gas are in the range 2×10^4–5×10^6 $M_\odot$, while the ratios between ionized and hot gas range from 10^{-4} to 7×10^{-3}. This result indicates that although in the ISM of these early-type galaxies a substantial amount of ionized gas is present, the hot ISM phase is by far its dominant component. This strengthens a posteriori the validity of the estimates of accretion rates derived considering only the high temperature gas.

References

Abraham, J., Aglietta, M., Aguirre, C., et al. 2007, Sci, 318, 938
Alexander, P. 2000, MNRAS, 319, 8
Allen, S. W., Dunn, R. J. H., Fabian, A. C., Taylor, G. B., & Reynolds, C. S. 2006, MNRAS, 372, 21
Anderson, J. M., & Ulvestad, J. S. 2005, ApJ, 627, 674
Anderson, J. M., Ulvestad, J. S., & Ho, L. C. 2004, ApJ, 603, 42
Auriemma, C., Perola, G. C., Ekers, R. D., et al. 1977, A&A, 57, 41
Baldwin, J. A., Phillips, M. M., & Terlevich, R. 1981, PASP, 93, 5
Balmaverde, B., & Capetti, A. 2006, A&A, 447, 97
Balmaverde, B., Capetti, A., & Grandi, P. 2006, A&A, 451, 35
Balmaverde, B., Baldi, R. D., & Capetti, A. 2008, A&A, 486, 119
Baum, S. A., & Heckman, T. 1989, ApJ, 336, 702
Becker, R. H., White, R. L., & Helfand, D. J. 1995a, ApJ, 450, 559
Becker, R. H., White, R. L., & Helfand, D. J. 1995b, ApJ, 450, 559
Best, P. N., Kauffmann, G., Heckman, T. M., et al. 2005a, MNRAS, 362, 25
Best, P. N., Kauffmann, G., Heckman, T. M., & Ivezić, Ž. 2005b, MNRAS, 362, 9
Buttiglione, S., Capetti, A., Celotti, A., et al. 2009a, A&A, 495, 1033
Buttiglione, S., Capetti, A., Celotti, A., & Chiaberge, M. 2009b, in preparation
Capetti, A., & Balmaverde, B. 2005, A&A, 440, 73
Capetti, A., & Balmaverde, B. 2006, A&A, 453, 27 (CB06)
Capetti, A., Kleijn, G. V., & Chiaberge, M. 2005, A&A, 439, 935
Capetti, A., Axon, D. J., Chiaberge, M., et al. 2007, A&A, 471, 137
Chiaberge, M., Capetti, A., & Celotti, A. 1999, A&A, 349, 77
Cohen, A. S., Lane, W. M., Cotton, W. D., et al. 2007, AJ, 134, 1245
Condon, J. J., Cotton, W. D., Greisen, E. W., et al. 1998, AJ, 115, 1693
Condon, J. J., Cotton, W. D., & Broderick, J. J. 2002, AJ, 124, 675
de Ruiter, H. R., Parma, P., Capetti, A., et al. 2005, A&A, 439, 487
de Zotti, G., Ricci, R., Mesa, D., et al. 2005, A&A, 431, 893
Falcke, H., Nagar, N. M., Wilson, A. S., & Ulvestad, J. S. 2000, ApJ, 542, 197
Fanti, C., Fanti, R., de Ruiter, H. R., & Parma, P. 1987, A&AS, 69, 57
Fanti, R., Gioia, I., Lari, C., & Ulrich, M. H. 1978, A&AS, 34, 341
Feretti, L., Giovannini, G., Gregorini, L., Parma, P., & Zamorani, G. 1984, A&A, 139, 55
Filho, M. E., Fraternali, F., Markoff, S., et al. 2004, A&A, 418, 429
Giovannini, G., Feretti, L., Gregorini, L., & Parma, P. 1988, A&A, 199, 73

Giovannini, G., Giroletti, M., & Taylor, G. B. 2007, A&A, 474, 409
Hardcastle, M. J., & Worrall, D. M. 2000, MNRAS, 314, 359
Hardcastle, M. J., Evans, D. A., & Croston, J. H. 2007, MNRAS, 376, 1849
Heckman, T. M. 1980, A&A, 87, 152
Hine, R. G., & Longair, M. S. 1979, MNRAS, 188, 111
Ho, L. C., & Ulvestad, J. S. 2001, ApJS, 133, 77
Ho, L. C., Filippenko, A. V., & Sargent, W. L. W. 1997, ApJS, 112, 315
Hummel, E., van der Hulst, J. M., & Dickey, J. M. 1984, A&A, 134, 207
Jackson, N., & Rawlings, S. 1997, MNRAS, 286, 241
Jansen, R. A., Fabricant, D., Franx, M., & Caldwell, N. 2000, ApJS, 126, 331
Jones, D. L., Wrobel, J. M., & Shaffer, D. B. 1984, ApJ, 276, 480
Kellermann, K. I., Pauliny-Toth, I. I. K., & Williams, P. J. S. 1969, ApJ, 157, 1
Kewley, L. J., Groves, B., Kauffmann, G., & Heckman, T. 2006, MNRAS, 372, 961
Kunert-Bajraszewska, M., & Thomasson, P. 2009, Astron. Nachr., 330, 210
Laing, R. A., Jenkins, C. R., Wall, J. V., & Unger, S. W. 1994, in The First Stromlo Symposium: The Physics of Active Galaxies, 1994, ed. G. V. Bicknell, M. A. Dopita, & P. J. Quinn, ASP Conf. Ser., 54, 201
Lynds, R. 1971, ApJ, 168, L87
Marcha, M. J. M., Browne, I. W. A., Impey, C. D., & Smith, P. S. 1996, MNRAS, 281, 425
Marchã, M. J. M., Browne, I. W. A., Jethava, N., & Antón, S. 2005, MNRAS, 361, 469
Martin, P. G., Angel, J. R. P., & Maza, J. 1976, ApJ, 209, L21
Miller, J. S. 1975, ApJ, 200, L55
Morganti, R., Ulrich, M.-H., & Tadhunter, C. N. 1992, MNRAS, 254, 546
Morganti, R., Oosterloo, T. A., Capetti, A., et al. 2003, A&A, 399, 511
Nagar, N. M., Wilson, A. S., Mulchaey, J. S., & Gallimore, J. F. 1999, ApJS, 120, 209
Nagar, N. M., Wilson, A. S., & Falcke, H. 2001, ApJ, 559, L87
Nagar, N. M., Falcke, H., Wilson, A. S., & Ulvestad, J. S. 2002, A&A, 392, 53
Nagar, N. M., Falcke, H., & Wilson, A. S. 2005, A&A, 435, 521
Osterbrock, D. E. 1989, Astrophysics of gaseous nebulae and active galactic nuclei (Research supported by the University of California, John Simon Guggenheim Memorial Foundation, University of Minnesota, et al. Mill Valley, CA, University Science Books, 1989, 422 p.)
Rawlings, S., & Saunders, R. 1991, Nature, 349, 138
Rawlings, S., Saunders, R., Eales, S. A., & Mackay, C. D. 1989, MNRAS, 240, 701
Readhead, A. C. S., Xu, W., Pearson, T. J., Wilkinson, P. N., & Polatidis, A. G. 1994, in Compact Extragalactic Radio Sources, ed. J. A. Zensus, & K. I. Kellermann, 17
Reynolds, C. S. 1997, MNRAS, 286, 513
Sadler, E. M., Jenkins, C. R., & Kotanyi, C. G. 1989, MNRAS, 240, 591
Snellen, I. A. G., Schilizzi, R. T., Miley, G. K., et al. 2000, MNRAS, 319, 445
Spinrad, H., Marr, J., Aguilar, L., & Djorgovski, S. 1985, PASP, 97, 932
Stanger, V. J., & Warwick, R. S. 1986, MNRAS, 220, 363
Torniainen, I., Tornikoski, M., Lähteenmäki, A., et al. 2007, A&A, 469, 451
Ulvestad, J. S., & Wilson, A. S. 1984, ApJ, 278, 544
Urry, C. M., & Padovani, P. 1995, PASP, 107, 803
White, R. L., & Becker, R. H. 1992, ApJS, 79, 331
Wrobel, J. M. 1991, AJ, 101, 127
Wrobel, J. M., & Heeschen, D. S. 1991, AJ, 101, 148
York, D. G., Adelman, J., Anderson, Jr., J. E., et al. 2000, AJ, 120, 1579